

# Hadronic Decays of Beauty and Charm from CLEO

Jorge L. Rodriguez  
(CLEO Collaboration)

*Department of Physics and Astronomy University of Hawaii  
2505 Correa Road Watanabe Hall 227  
Honolulu, Hawaii 96822*

**Abstract.** A selection of recent results on hadronic charm and beauty decays from the CLEO experiment are presented. We report preliminary evidence for the existence of final state interactions in  $B$  decays and the first observation of the decay  $B^0 \rightarrow D^{*+} D^{*-}$  with a branching fraction of  $(6.2_{-2.9}^{+4.0} \pm 1.0) \times 10^{-4}$ . We also present preliminary results on the first observation of the broad,  $J^P = 1^+$ , charmed meson resonance with a mass of  $m_{D_1(j=1/2)^0} = 2.461_{-0.034}^{+0.041} \pm 0.010 \pm 0.032$  GeV and a width of  $\Gamma = 290_{-79}^{+101} \pm 26 \pm 36$  MeV and branching fraction measurements of the  $B^- \rightarrow D_j^0 \pi^-$  decay. Finally, we report on our search for the radial excitation of a spin 1 charmed meson, the  $D^{*'+}$ , and on an improved measurement of the ratio of decay rates  $\Gamma(D^0 \rightarrow K^+ \pi^-) / \Gamma(D^0 \rightarrow K^- \pi^+)$ .

## INTRODUCTION

The CLEO experiment has provided important contributions to our understanding of hadronic decays of the beauty and charm systems since it began taking data in the early 1980s. The wealth of results is due primarily to the large data samples collected over the years and the excellent tracking, energy resolution and reasonably good particle ID of the CLEO series of detectors. In this paper we present five analyses on hadronic decays of charm and bottom mesons.

CLEO is currently analyzing data from two separate runs taken with different detector configurations. The first run ended in the Summer of 1995 and includes a total luminosity of  $3.1 \text{ fb}^{-1}$  on and  $1.6 \text{ fb}^{-1}$  taken 60 MeV below the  $\Upsilon(4S)$ . Given the  $B\bar{B}$  cross section this sample corresponds to 3.1 million  $B\bar{B}$  pairs. The configuration of the detector during the first run is described in detail in Ref. [1]. This dataset will be referred to as the CLEOII dataset hereafter. At the end of the CLEOII run the detector was significantly improved with the replacement of the inner straw tube drift chambers by a 3 layer silicon vertex (SVX) detector [2]. In addition, the argon-ethane gas in the drift chambers was replaced with

<sup>1)</sup> Unless otherwise indicated complex conjugate states are implied throughout this paper

a helium-propane mixture which improved both particle ID and the momentum resolution in the drift chambers. Finally, the track fitting software was updated to one based on the Kalman filtering algorithm. These improvements in tracking and particle ID, while featured in only two of the analysis presented here will become increasingly important in future analyses. The data collected and reconstructed, with the CLEOII upgrade, (CLEOII/SVX), consists of  $2.5 \text{ fb}^{-1}$  on and  $1.3 \text{ fb}^{-1}$  off resonance. The data run for CLEOII/SVX will be completed at the end of 1998.

## First Observation of $B^0 \rightarrow D^{*-} D^{*+}$

The Cabbibo suppressed decay  $B^0 \rightarrow D^{*-} D^{*+}$  is a potentially interesting CP violation mode, whose rate is expected to be comparable to the gold plated CP  $B^0 \rightarrow J/\Psi K_s$  decay. Since the  $D^{*+} D^{*-}$  final state can be obtained from either  $B^0$  or a  $\bar{B}^0$  this decay mode can be used to extract  $\sin 2\beta$  through  $B^0 \bar{B}^0$  mixing. The amplitude for this decay is dominated by the external tree diagram and we can estimate its rate by comparison to the measured  $B^0 \rightarrow D^{*-} D_s^{*+}$  rate, after taking into account the appropriate ratio of decay constants and CKM matrix elements. While the expected rate is of order 0.1 %, the rather large number of particles, six in the lowest multiplicity mode, in the decay chain significantly reduces the expected yield.

CLEO has performed a search for this mode by examining all of the currently available data collected on the  $\Upsilon(4S)$  [3]. This includes the complete CLEOII ( $3.1 \text{ fb}^{-1}$ ) and the available portion of CLEOII/SVX data ( $2.5 \text{ fb}^{-1}$ ). The decay chain is fully reconstructed cutting on kinematic variables to reduce backgrounds. In this analysis only three of the possible four combinations of the  $D^{*+} D^{*-}$  were used. The decay mode with two soft  $\pi^0$ , the  $B^0 \rightarrow (D^+ \pi^0)(D^- \pi^0)$  decays was not used due to background considerations. For events in the CLEOII/SVX sample an additional requirement was imposed to take advantage of the better position resolution obtained from the SVX.

The observables used to extract the signal were the beam-constrained mass ( $M_{BC}$ ) and the difference between the reconstructed energy and the beam energy ( $\Delta E$ ). At CLEO, the  $B$ s are produced nearly at rest so  $\Delta E$ , for real events, is peaked at zero while backgrounds from other decays peak one or more pion mass away from zero. The beam-constrained mass variable is just the usual invariant mass with the beam energy substituted for the measured energy. The resolution of  $M_{BC}$  is significantly better than the invariant mass, by about an order of magnitude, due to the small spread of the beam energy. In Figure 1 we show the scatter plots of the on- $\Upsilon(4S)$  distributions for events that pass all of event selection criteria. The solid rectangle in Figure 1 (left) is the signal region. A total of 4 events were observed.

To estimate the backgrounds that enter into the signal region, two independent methods were used. The first estimate is based on events in the  $\Delta E$  vs.  $M_{BC}$  sideband indicated by the region outside dashed rectangle in Figure 1 (left).

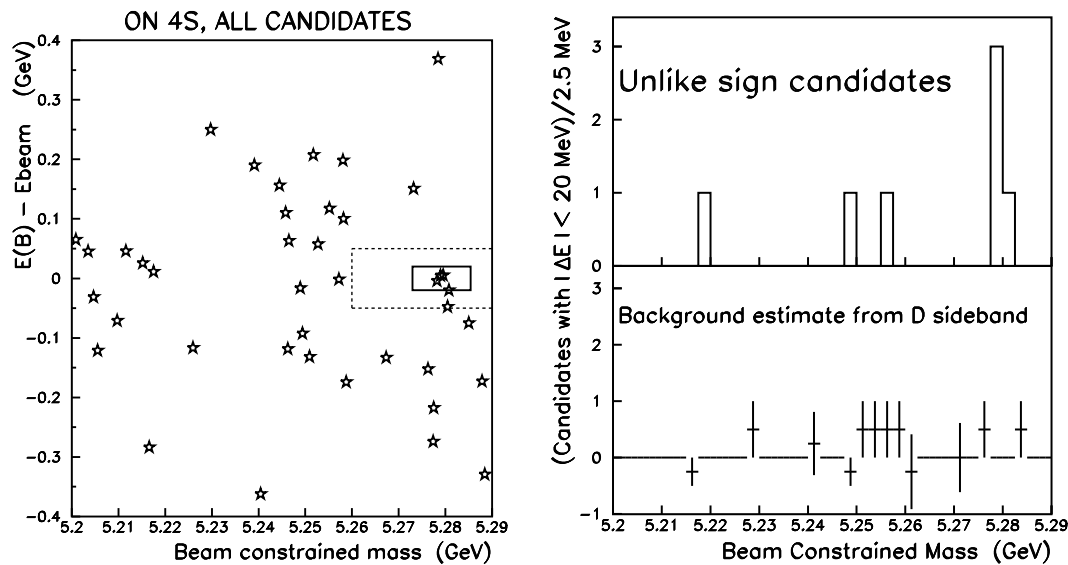


**FIGURE 1.** Scatter plot of on 4S events in  $\Delta E$  and  $M_{BC}$  (left). Beam-constrained mass distribution for events that lie within 20 MeV of 0.0 in  $\Delta E$  (right-top). The plot (right-bottom) shows the backgrounds from the  $D$  mass sidebands.

An estimate of  $0.26 \pm 0.04$  events is determined from this sideband estimate. A second estimate is obtained by adding contributions from continuum,  $B\bar{B}$  (other kinematically similar  $B$  decays that can fake the signal) and random combination that are reconstructed as signal. Each of these contributions were modeled by off-resonance data, Monte Carlo, and/or  $D$  mass sidebands. This estimate predicts a background of  $0.37 \pm 0.05$  events.

The branching fraction measured given the four observed events is:

$$\mathcal{B}(B^0 \rightarrow D^{*-} D^{*+}) = (6.2_{-2.9}^{+4.0} \pm 1.0) \times 10^{-4}. \quad (1)$$

This value is determined from an unbinned likelihood fit using the larger of the two background estimates. This value is consistent with the expected rate of 0.1% given the measured branching fraction of the  $B^0 \rightarrow D^{*-} D_s^{*+}$ , our knowledge of decay constants and the CKM matrix elements [3].

## Angular Distributions in $B \rightarrow D^* \rho$

A full partial wave analysis of the decays  $B^- \rightarrow D^{*0} \rho^-$  and  $\bar{B}^0 \rightarrow D^{*+} \rho^-$  has been performed using the entire CLEOII data sample. These decays proceed primarily through tree-level  $b \rightarrow c W$  emission and, to first order, the amplitude for the decays are independent of a CKM phase. The absence of a weak phase suggests a clean model to study the effects of final state interactions (FSI) in hadronic  $B$  decays.

The full partial wave decomposition, with its own phases, provides us with a way to determine the strong phases through an analysis of the angular distribution of the final states.

In order to extract information on the strong phases we first need to express the differential decay rate in terms of complex amplitudes and helicity angles. In this analysis we use the helicity basis expressed in three components; two, the  $H_{\pm}$ , represent the transverse components and one, the  $H_0$  describes the longitudinal component. Squaring and factoring the amplitude gives the differential decay rate in terms of the helicity amplitudes and the helicity angles  $\theta_{\rho}$ ,  $\theta_{D^*}$  and  $\chi$ . The form of the expression is,

$$\begin{aligned} \frac{d\Gamma}{d\cos\theta_{D^*}d\cos\theta_{\rho}d\chi} = & 4|H_0|^2 \cos^2\theta_{D^*} \cos^2\theta_{\rho} + (|H_-|^2 + |H_+|^2) \sin^2\theta_{D^*} \sin^2\theta_{\rho} \\ & + 2 \left[ \text{Re}(H_+H_-^*) \cos 2\chi - \text{Im}(H_+H_-^*) \sin 2\chi \right] \sin^2\theta_{D^*} \sin^2\theta_{\rho} \\ & + [\text{Re}(H_+H_0^* + H_-H_0^*) \cos \chi - \text{Im}(H_+H_0^* - H_-H_0^*) \sin \chi] \sin 2\theta_{D^*} \sin 2\theta_{\rho}. \quad (2) \end{aligned}$$

The two helicity angles are defined in the rest frame of the decay as the angle between one of the daughters and the direction of the parent in the rest frame of the  $B$ . The angle  $\chi$  is the angle between the two decay planes and is related to the azimuthal direction of the helicity axis by  $\chi = \phi_{D^*} - \phi_{\rho}$ . In the amplitude, the strong phase information is contained in the terms with the imaginary parts; in Equation (2), no FSI implies that either  $\text{Im}(H_+H_0^* - H_-H_0^*)$  and  $\text{Im}(H_+H_-^*)$  are zero, or conversely, that all amplitudes are relatively real [4].

All events are required to pass a series of selection criteria to fully reconstruct the decay chain of the  $B$  using three decay modes of the  $D^0$ , the  $K\pi$ ,  $K\pi\pi^0$  and  $K3\pi$ , and the dominant decay modes of the  $D^*$  [6]. Two methods are used to extract the phase information in Equation (2): a moments analysis [5] in which the components of each term in Equation (2) are extracted and a direct determination of the magnitude and phases of the helicity amplitudes from a three dimensional (3D) unbinned maximum likelihood fit of the data to the functional form in Equation (2).

In the unbinned likelihood fit and moments analysis the likelihood function includes terms for the signal and background contributions, factorizing each term into an angular part and a mass part. The mass part characterizes the  $\rho$  invariant mass with a relativistic Breit-Wigner and the beam-constrained mass with a Gaussian function. The angular part is modeled by Equation (2). To minimize the number of free parameters the fit is first performed ignoring the angular part and the parameters of the mass function are extracted. In the second step, the fit is redone including the angular function and fixing the mass parameters to values extracted from the first fit. The parameters in the angular part of the likelihood function are the phases and magnitudes of the transverse helicity amplitudes relative to the longitudinal component which is set to  $H_0 = 1$  and  $\delta_0 = 0$  in the fit. The amplitudes are then rescaled to satisfy the normalization condition  $|H_0|^2 + |H_-|^2|H_+|^2 = 1$ . The results of the likelihood fit for the strong phases and amplitudes are given in

Table 1. The coefficients of Equation (2) have also been determined from the fit and a comparison made with the values obtained from the moments analysis. We find that the results are consistent with each other within statistical errors (see Table 2). Our values for the phases in Table 1 suggest non-trivial strong phases in both the  $B^- \rightarrow D^{*0}\rho^-$  and  $\bar{B}^0 \rightarrow D^{*+}\rho^-$  modes, however the statistical size of our sample does not provide us with an independent confirmation of the results in a 1D fit of the data to the  $\sin \chi$  or  $\sin 2\chi$  distributions.

The results of the fit are also used to test the factorization hypothesis by comparing the polarization of the  $\bar{B}^0 \rightarrow D^{*+}\rho^-$  decay with the polarization in the semi-leptonic  $\bar{B}^0 \rightarrow D^{*+}l^-\bar{\nu}$  at the appropriate  $q^2$  scale. The predicted values for the longitudinal polarization in the semi-leptonic decay at  $q^2 = m_\rho^2$ , range from 85% to 88% and the recent CLEO results is  $91.4 \pm 15.2 \pm 8.9\%$  [6]. The longitudinal polarization from the fit is  $87.8 \pm 3.4 \pm 4.0\%$  consistent, within errors, with both the theoretical predictions and the semi-leptonic measurement.

**TABLE 1.** Phases extracted from the unbinned likelihood fit

Parameter	$B^0 \rightarrow D^{*+}\rho^-$	$B^- \rightarrow D^{*0}\rho^-$
$\delta_-$	$0.19 \pm 0.23 \pm 0.14$	$1.13 \pm 0.27 \pm 0.17$
$\delta_+$	$1.47 \pm 0.37 \pm 0.32$	$0.95 \pm 0.31 \pm 0.19$
$ H_- $	$0.317 \pm 0.052 \pm 0.013$	$0.283 \pm 0.068 \pm 0.039$
$ H_+ $	$0.152 \pm 0.058 \pm 0.037$	$0.228 \pm 0.069 \pm 0.036$

## Measurements in $B^- \rightarrow D_J^0\pi^-$

The  $L = 1, n = 1$  charmed mesons are the  $P$  wave orbital excitations in which four spin-orbit configurations are possible. In the heavy quark limit, these combinations can be identified by the  $j_l$  quantum number which couples the spin of the light quark with the orbital angular momentum. These states form two doublets: a  $j_l = 3/2$  and a  $j_l = 1/2$  which, from conservation of parity and angular momentum, decay via either  $S$  or  $D$  waves. In the heavy quark limit, the  $j_l = 1/2$  decays only via  $S$  wave while the  $j_l = 3/2$  can decay only via  $D$  wave. The only  $L = 1$  states so far observed have been the narrow  $L = 1, n = 1$  resonances, the  $D_1(2420)$  and the  $D_2^*(2460)$  with widths of order 20 MeV. These states have been assigned

**TABLE 2.** Coefficients in Equation (3) extracted from the likelihood fit

Coefficient	$B^0 \rightarrow D^{*+}\rho^-$		$B^0 \rightarrow D^{*+}\rho^-$	
	From L.L. fit	From moments	From L.L. fit	From moments
$H_0^2$	0.856	$0.751 \pm 0.073$	0.859	$0.626 \pm 0.074$
$H_+^2 + H_-^2$	$0.140 \pm 0.040$	$0.159 \pm 0.034$	$0.143 \pm 0.060$	$0.168 \pm 0.036$
$Im(H_-H_0^* - H_+H_0^*)$	$0.110 \pm 0.074$	$0.042 \pm 0.103$	$-0.071 \pm 0.109$	$-0.145 \pm 0.101$
$Re(H_-H_0^* + H_+H_0^*)$	$0.341 \pm 0.088$	$0.352 \pm 0.104$	$0.250 \pm 0.105$	$0.193 \pm 0.109$
$Im(H_+H_-^*)$	$0.053 \pm 0.021$	$0.057 \pm 0.024$	$-0.011 \pm 0.032$	$0.002 \pm 0.027$
$Re(H_+H_-^*)$	$0.023 \pm 0.024$	$0.018 \pm 0.023$	$0.068 \pm 0.029$	$0.043 \pm 0.025$

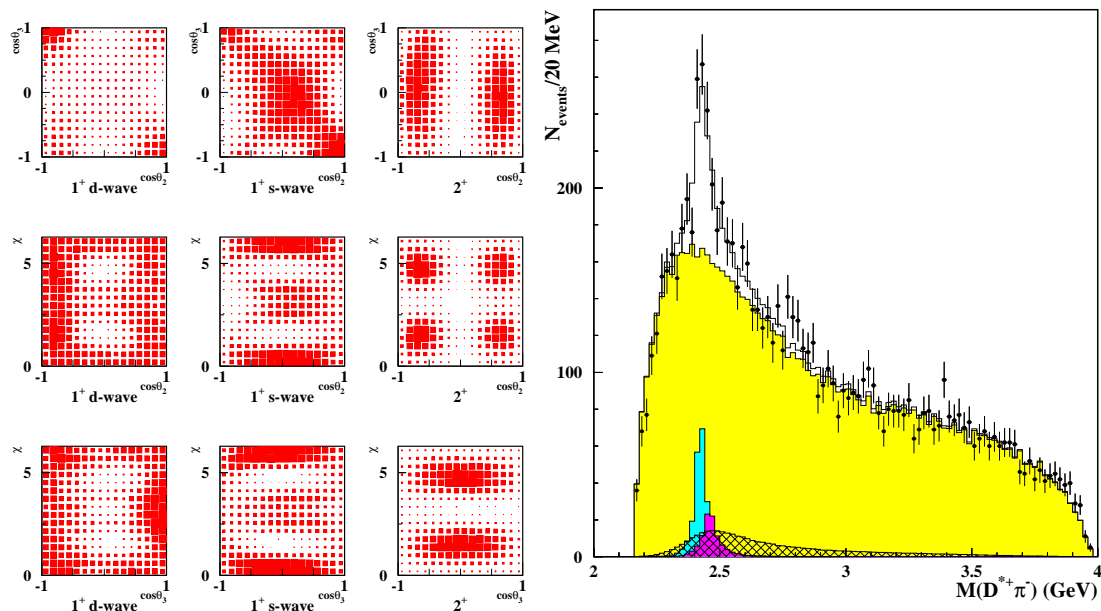


**FIGURE 2.** The reconstructed 2D angular distributions for the decays of the  $B^-$  meson to each of the three  $D_J^0$  resonances (left). The  $D^{*+}\pi^-$  invariant mass distribution for on 4S data with the 4D-MLF projections from each of the three  $D_J^0$  candidates, the two narrow  $1^+$  (light) and the  $2^+$  (darker) resonance and the broad  $1^+$  (cross-hatched) plus the total background are superimposed on the plot (right).

to the  $j_l = 3/2$  by observing the angular distributions of the decay products and measurements of the ratio of  $D^*\pi$  to  $D\pi$  decays in continuum production where the  $D_J$  are unpolarized.

A full partial wave analysis of the decay  $B^- \rightarrow D_J^0\pi_1^-, D_J^0 \rightarrow D^{*+}\pi_2^-, D^{*+} \rightarrow D^0\pi_3^+$  has been performed to measure the product branching fraction of the  $\mathcal{B}(B) \times \mathcal{B}(D_J)$  decays and the properties, the mass and width, of the broad  $D_1(j = 1/2)$  resonance. The measurements are extracted from a 4D unbinned maximum likelihood fit (4D-MLF) to the data, where the independent variables are the three helicity angles and the invariant mass of the  $D_J^0$  resonance.

An important point in this analysis is the fact that the  $D_J$  is completely polarized since it is the decay product of a pseudo-scalar decay to a vector plus another pseudo-scalar. Knowing the initial polarization of the  $D_J$  and the fact that angular momentum and parity are both conserved provides us with a clear picture, in the heavy quark limit, of the angular decay distribution in final states that first decay through one of the three intermediate  $D_J^0$  resonances. In other words, we can distinguish among the three possible  $L = 1$  states, those that decay to a  $D^{*+}\pi^-$ , not only by using the invariant mass but also by examining the full angular distribution of the final state.

A partial reconstruction technique selects the events from among the entire CLEOII dataset. These events are used in the fit to the 4D maximum likelihood

function. In the partial reconstruction method the entire decay is reconstructed, up to a quadratic ambiguity, from the 4-momenta of the three pions ( $\pi_1, \pi_2, \pi_3$ ) in the decay chain and imposing energy-momentum conservation at each decay vertex [9]. This method improves statistics by about an order of magnitude over the usual full reconstruction technique since it eliminates the explicit reconstruction of the charmed meson. A trade off to the gain in statistics comes from the increased complexity of the analysis and higher levels of backgrounds. These backgrounds are however, modeled by using the  $1.6 \text{ fb}^{-1}$  of off-resonance data and Monte Carlo simulations. In Figure 2 (left) we show the  $D^{*+}\pi^-$  invariant mass distribution taken from events that pass the selection criteria described in Ref. [10] in the on-resonance CLEOII dataset. Superimposed on the plot are the  $D^{*+}\pi^-$  invariant mass projection from the 4D-MLF for each of  $D_J^0$  candidates plus the total background contribution from various sources; continuum and other  $B\bar{B}$  decays with similar kinematics. The ability of the angular information to distinguish between the three possible resonances is illustrated in Figure 2 (right) where Monte Carlo simulations of the  $B^-$  decays to each of the three  $L = 1$   $D_J$  resonances are shown.

The 4D likelihood function used in the fit includes terms for the angular distribution, mass amplitudes of the resonances, strong phase shifts and parameters that allow for mixing between the two  $1^+$  states. It also allows for detector smearing and acceptance. The functional form of the amplitude is

$$\begin{aligned} \mathcal{A}_{B \rightarrow D^{*+}\pi^-\pi^-} = & \alpha_{nr} e^{i\delta_{nr}} + \alpha_2 A_2 a_2 e^{i\delta_2} + \alpha_{1n} A_{1n} (a_{1d} \cos \beta + a_{1s} \cos \beta e^{i\phi}) \\ & + \alpha_{1b} A_{1b} (a_{1s} \cos \beta - a_{1d} \cos \beta e^{i\phi}) e^{i\delta_1} \end{aligned} \quad (3)$$

where the  $\alpha_i$  allows for different contributions from the various resonant and non-resonant  $D^{*+}\pi^-\pi^-$  components, the  $A_i$  are Breit-Wigner amplitudes, and the  $a_i$  are the angular ( $D_{m,m'}^j$ ) amplitudes. The mixing between the narrow and broad  $1^+$  resonances is currently described by the mixing angles  $\beta$  and  $\phi$  and the strong phases for the resonant and non-resonant components are included via the  $\delta$  parameters. The  $1n, 2, 1b$ , and  $nr$  subscripts refer to the narrow  $1^+, j_l = 3/2$  and  $2^+, j_l = 3/2$  resonances, the broad  $1^+, j_l = 1/2$  resonance and the non-resonant component respectively. This parameterization is not unique and an alternative parameterization has been used as a systematic check. The variation in the results due to the alternative parameterization is quoted as an additional systematic error. The fit is performed with the mass and width of the relativistic Breit-Wigners for the narrow  $2^+$  and the  $1^+$  states fixed to their measured values [7]. The normalization of each of the three resonant and the non-resonant components plus the mass and width of the broad  $1^+$  state are allowed to float in the fit. From the fit we extract the invariant mass and width of the broad  $1^+$  resonance to be:

$$\begin{aligned} M_{D_1(j=1/2)^0} &= 2.461_{-0.034}^{+0.041} \pm 0.010 \pm 0.032 \quad \text{GeV} \\ \Gamma_{D_1(j=1/2)^0} &= 290_{-79}^{+101} \pm 26 \pm 36 \quad \text{MeV} \end{aligned} \quad (4)$$

where the first error is the statistical uncertainty, the third is the uncertainty from the parameterization of the amplitude and the second is the systematic uncertainty

from all other sources. From the 4D fit we also extract the product branching ratios of the  $B^-$  to each of the three  $D_J^0$  plus a single pion. These results are given in Table 3 together with the yields and the  $B^-$  branching fractions using the  $D_J^0$  branching fractions from isospin symmetry. The second systematic error in Table 3 represents the uncertainty in the parameterization of the grand-amplitude. These results are consistent with the values obtained earlier using a simpler 2D-MLF where not all of the angular information was used [10]. These branching fraction measurements, however, disagree with theoretical expectations from heavy quark effective theory which predict the rates to be about three times smaller than the our results [11]. Our preliminary results on the mass and width of the broad  $1^+$  charmed meson are in agreement with the quark model [12].

## Search for First Radial Excitations in Charmed Meson

In 1997 the DELPHI collaboration claimed evidence for the  $1^{st}$  radially excited charmed meson  $D^{*+}$  [8]. They found an excess of  $66 \pm 14$  events in their sample of reconstructed  $D^{*+}\pi^-\pi^+$  with a mass of  $2637 \pm 2 \pm 6$  MeV and a small width. The assignment of the quantum numbers was based primarily on the mass measurement which is consistent with theoretical expectations for a  $D^{*+}$  [13]. The width of the bump is approximately equal to the detector resolution so DELPHI sets an upper bound on the decay width of the  $D^{*+}$  to be  $< 15$  MeV at the 95% confidence level. The OPAL experiment has also performed a search for the  $D^{*+}$  in the same final state and in the DELPHI mass window using a similar analysis procedure. They however, found no excess and set an upper limit on  $D^{*+}$  production of  $f_{Z^0 \rightarrow D^{*+}} \times \mathcal{B}(D^{*+} \rightarrow D^{*+}\pi^-\pi^+) < 2.1 \times 10^{-3}$  95% C.L. [14]. Both experiments collect data at the  $Z^0$  mass so  $D^{*+}$  production is from the  $c\bar{c}$  and/or  $b\bar{b}$  continuum. Both experiments also estimate that about half of their candidates are from  $c\bar{c}$  production.

The analysis procedures used at CLEO are similar to those employed by both DELPHI and OPAL. First pion and kaon candidates are selected from tracks originating at the IP. These are then combined to form  $D^0$  and  $D^{*+}$  candidates requiring consistency with particle ID and that the invariant masses be within the nominal values. To test the reconstruction procedure and reduce the systematic errors, the

**TABLE 3.** Results of the 4D maximum likelihood fit to the decay  $B^- \rightarrow D_J^0\pi^-$

$B$ Decay Mode	Event Yield	$\mathcal{B}(B^- \rightarrow D_J^0\pi^-)^a \times 10^{-3}$	$\mathcal{B}(B^-) \cdot \mathcal{B}(D_J^0) \times 10^{-4}$
$D_1^0(j_l = 1/2)\pi^-$	$237.1 \pm 42$	$1.59 \pm 0.29 \pm 0.26 \pm 0.03 \pm 0.035$	$10.6 \pm 1.9 \pm 1.7 \pm 2.3$
$D_1(2420)^0\pi^-$	$420.0 \pm 41$	$1.04^{+0.27}_{-0.21} \pm 0.17 \pm 0.02 \pm 0.07$	$6.9^{+1.8}_{-1.4} \pm 1.1 \pm 0.4$
$D_2^*(2460)^0\pi^-$	$109.5 \pm 26$	$1.55 \pm 0.42 \pm 0.23 \pm 0.03 \pm 0.14$	$3.1 \pm 0.84 \pm 0.45 \pm 0.28$
$D^{*+}\pi^-\pi^-$	$160.0 \pm 61$	$9.7 \pm 3.6 \pm 1.5 \pm 1.9$	
Total		$29.2 \pm 4.5 \pm 3.7 \pm 3.1$	

<sup>a</sup> We use the  $D_J$  branching fraction assumed in much of the literature  $\mathcal{B}(D_1^0 \rightarrow D^{*+}\pi^-) = 2/3$  and  $\mathcal{B}(D_2^{*0} \rightarrow D^{*+}\pi^-) = 0.2$



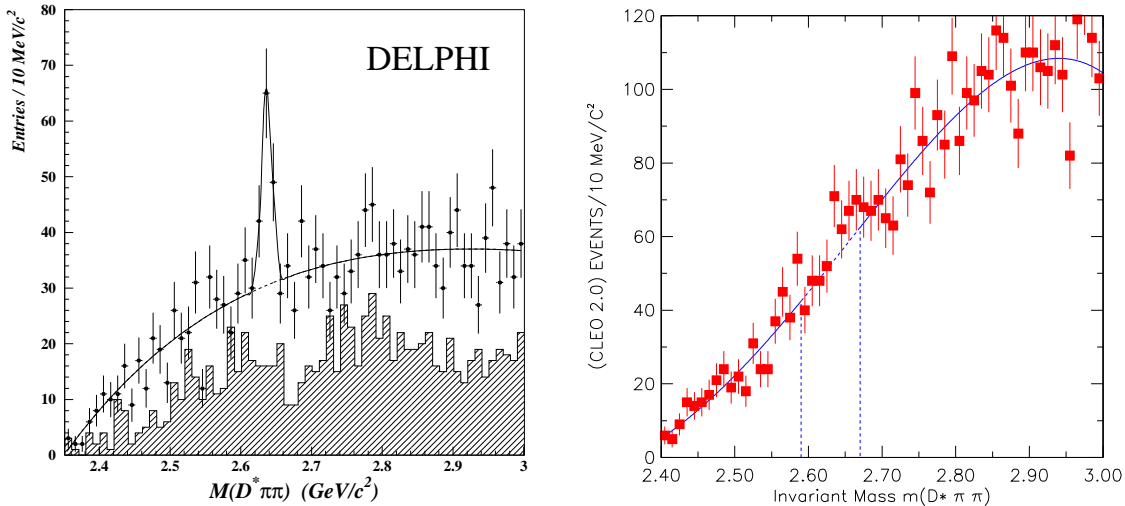


FIGURE 3. The  $D^{*+}\pi^-\pi^+$  invariant mass distribution from DELPHI (left), from CLEO (right).

$D^{*+}$  yields are compared to  $D_j^0$  yields since the reconstruction procedures differ only by a single charged pion. Also, the  $D^{*+}$  to  $D_j^0$  production ratio allows for a more direct comparison between the LEP and the CLEO results.

Using the entire CLEOII data set we have searched for the  $D^{*+}$  in the mass region suggested by the DELPHI results. We find no evidence of an excess the region between 2590 MeV and 2670 MeV, and set a preliminary upper limit of:

$$\frac{N_{D^{*+}} \cdot \mathcal{B}(D^{*+} \rightarrow D^{*+}\pi^-\pi^+)}{N_{D_2^{*0}} \cdot \mathcal{B}(D_2^{*0} \rightarrow D^{*+}\pi^-) + N_{D_1^0} \cdot \mathcal{B}(D_1^0 \rightarrow D^{*+}\pi^-)} < 0.16 @ 90\% \text{ C.L.} \quad (5)$$

This may be compared with the DELPHI measurement of  $0.49 \pm 0.18 \pm 0.10$  for this rate [8]. The invariant mass distributions from DELPHI [8] and CLEO are shown in Figurejrod:fig:dstrpime). The DELPHI result includes both  $b\bar{b}$  and  $c\bar{c}$  production.

## Measurement of $D^0 \rightarrow K^+\pi^-$ Decays

The decay  $D^0 \rightarrow K^+\pi^-$  can proceed either a through doubly Cabbibo suppressed decay (DCSD) channel or through  $D^0 - \bar{D}^0$  mixing. In the standard model, the rate is expected at 0.3% level so this decay can be used to search for exotic or beyond-standard model decay mechanisms. Standard model predictions for  $R$ , defined as  $R = \Gamma(D^0 \rightarrow K^+\pi^-) / \Gamma(D^0 \rightarrow K^-\pi^+)$ , from mixing vary considerably from about  $10^{-3}$  to  $10^{-10}$ . The contributions to  $R$  from DCSD is of order  $\tan^4 \theta_C \sim 3 \times 10^{-3}$  [15]. To separate the mixing and DCSD contributions a measurement of the decay time distribution is required. With the new silicon vertex detector, CLEO can now perform this measurement, however, in the discussion that follows we present only

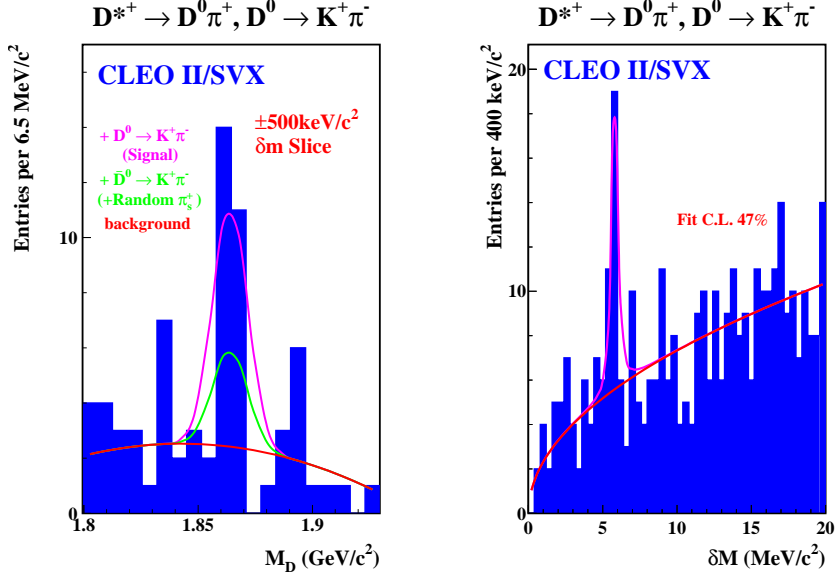


**FIGURE 4.** The wrong sign  $M_{D^0}$  and  $\delta M$  distributions with the results of the 1D-ML fit with the signal and background contributions superimposed on the data.

an  $R$  measurement that includes contributions from both mixing and DCSD. We plan to eventually add the time-dependent measurement to this analysis.

To measure the ratio  $R$  we have to determine the decay rates  $\Gamma(D^0 \rightarrow K^+\pi^-)$  and  $\Gamma(D^0 \rightarrow K^-\pi^+)$ . These rates are extracted from analyzing high momentum continuum  $D^{*+} \rightarrow D^0\pi_s^+ \rightarrow (K\pi)\pi_s^+$  events, where the sign of the slow pion ( $\pi_s^+$ ) tags whether the  $K\pi$  combination comes from a  $D^0$  or a  $\bar{D}^0$ . The combination where the sign of the  $K$  and the slow pion ( $\pi_s^+$ ) are the same is referred to as the “wrong sign” combination while events where the  $K$  and the  $\pi_s^+$  have opposite signs is referred to as the “right sign” combination. The wrong/right sign signal yields are determined by fitting the distribution of mass differences ( $\delta M$ ) between the  $D^{*+}$  and the  $D^0$  and requiring the  $D^0$  invariant mass ( $M_D$ ) to be within  $\pm 13$  MeV ( $2\sigma$ ) of the nominal  $D^0$  mass. An important feature in this analysis is the small width of both the  $M_D$  and  $\delta M$  mass distributions as compared to other experiments. This is due primarily to the improvements in the tracking algorithm and the vertex resolution of the SVX detector. For example, in the CLEOII/SVX data the resolution of  $M_D$  is now 6.5 MeV, while the  $\delta M$  resolution is 200 keV compared with the CLEOII pre re-processed (data reconstructed prior to the application of the Kalman algorithm) values of about 12 MeV and 750 keV respectively. The improved mass resolution allows for a greater separation of signal from backgrounds. This improvement is evident in the low levels of backgrounds in Figure 4.

Because of the rarity of the  $D^0 \rightarrow K^+\pi^-$  events, a significant amount of work has been done to both reject and understand the backgrounds which enter the  $M_D$  and  $\delta M$  distributions. The most significant background components are due to real  $\bar{D}^0 \rightarrow K^+\pi^-$  combined with a random slow  $\pi_s^+$  and backgrounds from  $D^{*+} \rightarrow (K^+\pi^-)\pi_s^+$  where the kaon and the pion are mis-identified. The random

slow  $\pi_s^+$  background tends to peak in the  $D^0$  mass region but not in  $\delta M$ , while the doubly mis-identified background tends to peak in  $\delta M$  but not in the  $D^0$  mass. The latter is reduced by forming the  $m_{\text{ap}}(D^0)$ , where the mass assignments to the kaon and pion are switched, vetoing the event if it's "mass-flip" mass is within  $4\sigma$  of the nominal  $D^0$  mass. The remaining backgrounds are modeled by Monte Carlo simulations. The background distributions are used in the likelihood function for the 1D maximum likelihood fit.

The preliminary result of the 1D ML fit for the ratio of decay rates is:

$$\frac{\Gamma(D^0 \rightarrow K^+\pi^-)}{\Gamma(D^0 \rightarrow K^-\pi^+)} = 0.0032 \pm 0.0012 \pm 0.0015 \quad (6)$$

This result was obtained from an analysis of the current CLEOII/SVX dataset which includes both the off and on-resonance samples for a total of  $3.8 \text{ fb}^{-1}$ . The new result is already more statistically significant, by itself, than the current world average of  $0.0072 \pm 0.0025$  [7]. There is currently about a factor of two more CLEOII/SVX data yet to be analyzed so we expect the statistical significance to improve. We are also working on improving the estimate of the systematic error and expected it to be much smaller than the value quoted in Equation (6). Finally, it is worth noting that while compatible, within errors, with the world average, the new  $R$  measurement is lower by about a factor of two and therefore more consistent with theoretical expectations.

## Summary and Conclusions

We have presented preliminary results from five CLEO analysis in hadronic decays of bottom and charmed mesons. From the  $B$  hadronic analyses we have shown results which provide us with the first observation and measurements of the decay  $B^0 \rightarrow D^{*-}D^{*+}$ , a first hint of final state interactions in  $B$  decays and a measurement of the decay rates of the  $B^-$  meson decaying into three of the  $L = 1$  charmed mesons plus a single pion. From the  $B^- \rightarrow D_J^0\pi^-$  analysis we have the first observation of the broad  $L = 1, j_l = 1/2$  charmed meson and have determined its mass and decay width. Our preliminary search for the first radial excitation of the charmed meson (the  $D^{*+}$ ) has been unable to confirm the observation by the DELPHI collaboration. Finally, our preliminary results on a measurement of the ratio  $\Gamma(D^0 \rightarrow K^+\pi^-)/\Gamma(D^0 \rightarrow K^-\pi^+)$  gives a results lower than previous measurements. This new measurement is an improvement over the previous CLEO results with a substantial increase in data and improved detector.

## REFERENCES

1. Y. Kubota, *et al.*, (CLEO Collaboration), *Nucl. Inst. Meth.*, **A320**, 66 (1992)
2. J. Alexander, *et al.*, *Nucl. Inst. Meth.*, **A326**, 243 (1993)

3. D. E. Jaffe, *et al.*, (CLEO Collaboration), *CLEO conference report* CLEO CONF98-07/ICHEP98-849 (1998). Submitted to *Phys. Rev. Lett.*
4. G. Kramer, T. Mannel, and W.F. Palmer, *Z. Phys.*, **C55**, 497 (1992)
5. A. Dighe, I. Dunietz and R. Fleischer, CERN preprint CERN-TH-98-85/hep-ph/9804253
6. G. Bonvicini *et al.*, (CLEO Collaboration), *CLEO conference report* CLEO CONF98-23/ICHEP9-852 (1998)
7. C. Caso *et al.*, (Particle Data Group), *Eur. Phys. J.*, **C3** (1998)
8. P. Abreu *et al.*, (DELPHI Collaboration), *Phys. Lett. B*, **426**, 231 (1998)
9. A description of the partial reconstruction technique as applied to a similar mode can be found in G. Brandenburg *et al.*, (CLEO Collaboration), *Phys. Rev. Lett.*, **80**, 2762 (1998)
10. J. Gronberg *et al.*, (CLEO Collaboration), *CLEO conference report* CLEO CONF96-25/ICHEP96 PA05-69 (1996)
11. M. Neubert, *Phys. Lett. B*, **418**, 173 (1998): hep-ph/9709327
12. S. Godfrey and R. Kokoski, *Phys. Rev. D*, **43**, 1679 (1991)
13. S. Godfrey and N. Isgur, *Phys. Rev. D*, **32**, 189 (1985)
14. OPAL Collaboration, *OPAL conference report* OPAL PN352/ICHEP98-1037 (1998)
15. D. Cinabro *et al.*, (CLEO Collaboration) *Phys. Rev. Lett.*, **72**, 1406 (1994)